Trimethyl Acetate on TiO_2(110): Preparation and Anaerobic Photolysis

J. M. White and Michael A. Henderson*

Interfacial Chemistry and Engineering Group, Pacific Northwest National Laboratory, Richland, Washington 99353

Received: February 23, 2005; In Final Form: April 25, 2005

The preparation and anaerobic ultraviolet photolysis of trimethyl acetate (TMA) on rutile TiO_2(110) have been examined with an emphasis on reaction paths. Substrates for photolysis were prepared by dosing trimethyl acetic acid at 100, 300, and 550 K. The chemistry was characterized by mass spectrometry during dosing and by H_2O adsorption and temperature programmed desorption (TPD) after dosing. Using TPD after photolysis and mass spectrometry during photolysis, the products ejected and retained during photolysis were sought. The photolysis results are interpreted using the following mechanistic model. Photons with energies exceeding 3 eV create electron−hole pairs in the substrate. With probabilities of 10^{-5} or lower, the holes initiate TMA chemistry by extracting an electron from the π orbital of the carboxylate moiety. The accompanying electrons are trapped at the surface and inhibit subsequent events of this chemistry. The electron-deficient intermediate, TMA*, decarboxylates to form CO_2 and either chemisorbed *tert*-butyl ($-C(CH_3)_3$) or physisorbed *i*-butene. For photolysis at 100 or 200 K, the $-C(CH_3)_3$ accumulates and there is a slow photon-driven secondary reaction that, with a source of H, hydrogenates adsorbed *tert*-butyl to physisorbed *i*-butane. For photolysis at 300 K, $-C(CH_3)_3$ thermally reacts to form and desorb *i*-butene and *i*-butane during photolysis.

1. Introduction

Research dealing with photochemical reactions on semiconductor oxides continues to be vigorously pursued.[1−3] There are many fundamental questions regarding the behavior of photon-mediated processes, and answering them can be valuable in engineering viable applied systems that convert photon energy to chemical energy or electrical energy. Examples include the splitting of water to produce H_2,[3] degradation of organic pollutants,[2] production of hydrophilic coatings,[4] disinfection of bacteria-contaminated surfaces,[5] and use of solar cells.[6]

This paper, one of a series,[7−11] reports on the photochemistry of a model system involving a well-characterized prototypical single-crystal oxide surface, rutile TiO_2(110), with a relatively small organic functional group, trimethyl acetate ($(CH_3)_3CCOO^-$, TMA), and irradiating it with ultraviolet photons. Prior work, focused on thermal chemistry, shows that after dosing trimethyl acetic acid ($(CH_3)CCOOH$, TMAA) the ensuing temperature programmed desorption (TPD) is dominated by CO, *i*-C_4H_8 (isobutene) *i*-C_4H_{10} (isobutane), and TMAA, and that after heating to 750 K the surface is free of carbon-containing species.[7]

The photochemistry is monitored using isothermal mass spectrometry (ISOMS) during irradiation and by comparing TPD spectra for irradiated and unirradiated adsorbate-covered surfaces. Previous publications have shown by scanning tunneling microscopy (STM) that TMA, formed by dosing TMAA to saturation at 300 K forms an ordered (2×1) array of chemisorbed species.[9−11] This saturated surface is very hydrophobic.[8] Consistent with the known chemistry of organic acids on titania, the adsorbate is identified as trimethyl acetate (TMA), the deprotonated form of TMAA.[12] The proton attaches to a nearby bridging oxygen anion. Photolysis of the as-dosed TMA−TiO_2(110) surface removes TMA species: CO_2 and isobutene (*i*-C_4H_8) dominate the ISOMS profiles; features ascribed to TMA groups (on Ti^{4+} rows) disappear in STM images, and new features appear on the oxygen vacancy rows; an electron energy loss spectroscopy (EELS) transition, identified as Ti^{3+}, grows with photolysis time; and TPD after irradiation indicates partial loss of TMA species.[10,11] As photolysis proceeds (under anaerobic conditions), the product formation rate quenches much more rapidly than can be accounted for by the removal of TMA species. Dosing the quenched surface with O_2 in the absence of photons removes the Ti^{3+} EELS signal and, after evacuation of O_2, a high photolysis rate returns and decays as the Ti^{3+} signal grows in again.[9,10] By dosing the surface with O_2 during photolysis, quenching is reduced and sustainable removal of TMA occurs.[13] As the TMA coverage drops, the hydrophilicity of TiO_2(110) is restored.[8]

Here, the focus is on the operative reaction paths for surfaces dosed with TMAA at selected temperatures from 100 to 550 K and photolyzed under anaerobic conditions at selected nominal temperatures between 100 and 300 K. A subsequent paper will deal with photolysis in the presence of O_2.[13] Photolysis at 100 K, where little desorbs during photolysis, provides evidence for prompt photochemical conversion of TMA to form physisorbed CO_2 and chemisorbed $C(CH_3)_3$, the latter reacting during subsequent TPD to release *i*-C_4H_8 and *i*-C_4H_{10} between 190 and 300 K. Further photolysis leads to steady accumulation of *i*-C_4H_{10} that appears as a desorption-limited product at 150 K in TPD. Complementary photolysis experiments at 200 and 300 K are presented for comparison. The initial specific rate (rate per TMA) of photon-driven CO_2 production photolysis after a 550 K dose is lower by a factor of 2.5 than photolysis after a 300 K dose.

The text below is arranged as follows: After describing the experimental apparatus in section 2, the preparation of adsorbate−

* Corresponding author. E-mail: ma.henderson@pnl.gov. Phone: (509) 376−2192.

10.1021/jp050944g CCC: $30.25
Published on Web 06/02/2005

substrate systems used in the photolysis is described in section 3. This section presents what is known about the structures formed by dosing TMAA at 100, 300, and 550 K. Section 4 describes the results obtained by photolyzing the as-dosed surfaces. TPD spectra with and without photolysis are compared in section 4.1, and ISOMS spectra are described in section 4.2. A phenomenological description of the reaction paths is presented in section 5 followed by a summary in section 6.

2. Experimental Section

The ultrahigh vacuum (UHV) apparatus, gas handling system, and sample preparation procedures have been described previously.[7,14] The TiO_2(110) substrate, attached to a liquid nitrogen cooled support, was cleaned routinely by cycles of Ar^+ sputtering and, to restore surface order, annealing to 850 K, typically for 10 min. The latter process is accompanied by the production of a small and reproducible concentration of oxygen vacancies evidenced by dissociating water. For the experiments reported here, the surface oxygen vacancy concentration was 7 $\pm$ 1%. Thus, nominally, there are 3.6×10^{13} bridging oxygen atom vacancies/cm^2, since a perfect TiO_2(110) surface exposes 5.2×10^{14} Ti^{4+} and bridging O^{2-} species/cm^2.[15]

With the clean and annealed substrate held at a selected temperature, TMAA was dosed through a pinhole doser connected to a 4 mm i.d. doser tube that terminated 1 mm from the substrate surface, thereby maximizing the probability that TMAA entering the chamber collides first with the sample surface. After dosing, the doser tube was retracted and the substrate rotated to align its surface normal with the direction of the incident photon flux. With a few exceptions, UV photons from a 100 W high-pressure mercury arc, focused and filtered through H_2O to remove infrared photons, were directed through a quartz window onto the TMA-covered surface. At the sample, this source provides about 10^{17} photons/s,[16] having energies exceeding the 3.2 eV band gap of TiO_2.[15] To keep the temperature rise during irradiation below 6 K, a rotating chopper wheel (photons blocked 84% of the time) was employed in many experiments. When the source was not chopped, the sample temperature, measured with a thermocouple attached to the edge of the TiO_2 crystal, rose as much as 30 K during 10 min of photolysis. Late in the series of experiments, a fiber optic was added and, for a few experiments, was used to direct the UV photons onto the substrate. This fiber passed from an external lens focusing device through the vacuum wall and ended within 1 cm of the substrate surface. The photon flux entering the chamber was 20% of the above configuration, that is, 2×10^{16} photons/s.

Products were detected by quadrupole mass spectrometry before, during, and after photolysis. During dosing or photolysis, the products ejected were monitored by ISOMS with the TiO_2 surface normal positioned to align with the doser axis or the incident photon direction—both 45° away (in opposite directions) from the cylinder axis of the quadrupole mass spectrometer (QMS). Before and after photolysis, TPD spectra (nominally 2 K s^{-1} ramp rate) were taken with the substrate surface normal aligned with the cylinder axis of the apertured QMS. To compare relative amounts of material detected during TPD with amounts detected during either photolysis or dosing, the response of the quadrupole detector was determined by measuring TPD spectra for TMA-saturated surfaces with two orientations—the normal TPD position and the normal photolysis position.

To quantify the relative amounts of desorbing products, ion intensity profiles in the time domain were adjusted systematically for background responses and, after accounting for fragmentation patterns, were integrated.[7] Fragmentation patterns were measured for TMAA, *i*-C_4H_8, *i*-C_4H_{10}, CO_2, and CO and taken from the literature for other candidate species. To convert the integrated areas associated with the products to absolute amounts (species/cm^2), we directly dosed adsorbates so that, in subsequent TPD, the monolayer peaks were saturated. The integrated intensity versus time curves provide calibrated monolayer peak areas, and making use of either literature measurements of absolute saturation coverage or estimates based on liquid-phase densities, these peak areas were used to convert monolayer intensities to molecules/cm^2. Taking account of instrument drift over week-long time scales, uncertainties arising from background subtractions, and uncertainties in the coverages corresponding to monolayers, the estimated uncertainties in these numbers are as high as $\pm$15%.

3. Sample Preparation

The samples for photolysis were prepared by dosing TMAA onto clean surfaces, with the latter prepared by annealing at 850 K for 300 s in a vacuum. The substrates were held at 100, 300, or 550 K during TMAA dosing. While the thermal chemistry during and following doses at 100, 300, and 550 K has been discussed in an earlier publication,[7] a brief synopsis is given in this section, supplemented by additional material that is germane to the subsequent photochemistry. In section 4, some additional thermal chemistry data are presented in the context of comparing TPD with and without photolysis. In the following, 1 ML is defined as 5.2×10^{14} cm^{-2}, the number of exposed Ti^{4+} sites/cm on a perfect TiO_2(110) surface.

Among the many ions tracked in various experiments, those presented here are diagnostic for identified neutral species leaving the adsorbate−vacuum surface. For example, 41 amu, $C_3H_5^+$, is typically a relatively intense fragment of those organic molecules containing three or more carbon atoms that are plausible products. Thus, in TPD, the 41 amu trace identifies peak temperatures of any of these species. At each peak temperature, the desorbing species is identified using other ion fragments in conjunction with known fragmentation patterns. In this context, the 57 amu, $C_4H_9^+$, is diagnostic for TMAA; 43 amu, $C_3H_7^+$, for *i*-C_4H_{10}; and 56 amu, $C_4H_8^+$, for *i*-C_4H_8. Other ions, that is, 2 amu, H_2^+; 16 amu, CH_4^+; 18 amu, H_2O^+; 28 amu, CO^+; and 44 amu, CO_2^+, were tracked to search for H_2, CH_4, H_2O, CO, and CO_2.

Preparation at 300 K. Typically, TPD spectra following doses at 300 K were initiated after terminating the dose and cooling the substrate to 100 K. Since 300 K lies well above the multilayer and chemisorbed TMAA peaks at 190 and 235 K,[7] these do not appear and the profiles begin to rise only at 300 K. As shown below, some of the profiles rise rather sharply and are, thus, relatively sensitive to small time and temperature variations during dosing. On the basis of calibrated TPD spectra, the calculated sum of TMAA and C_4 products desorbing from a saturated substrate is 0.6 $\pm$ 0.1 ML, slightly higher than the TMA coverage based on STM data (0.5 ML). While the difference lies within the limit of our estimated uncertainty, there is in TPD as much as 0.1 ML of weakly adsorbed TMAA desorbing between 300 and 400 K. These species may readily migrate across the surface and not appear in STM images. If so, the coverage measured by STM would be slightly lower than that measured by TPD. The surface formed by dosing at 300 K is very hydrophobic;[8] submonolayer doses of H_2O at 100 K desorb with an onset at 135 K, characteristic of bulk water sublimation.

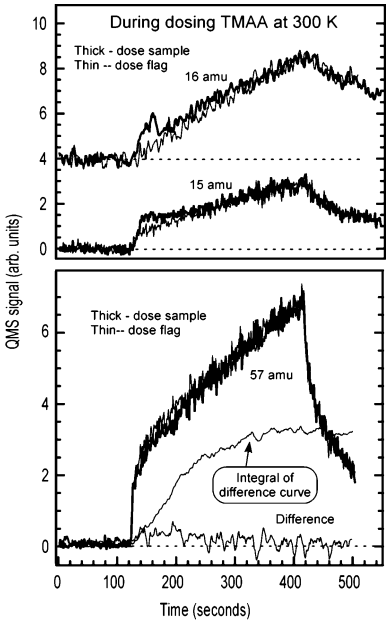

Figure 1. Isothermal mass spectrometry (ISOMS) during the dosing of trimethyl acetic acid (TMAA) onto an annealed clean rutile TiO_2-(110) surface held at 300 K (thick line) and onto an inert flag held at 300 K and placed between the rutile substrate and the doser tube exit (thin line). Along the time axis, the doses began at 120 s and ended 300 s later at 420 s. The 57 amu difference curve and the integral of the difference curve are shown in the lower panel.

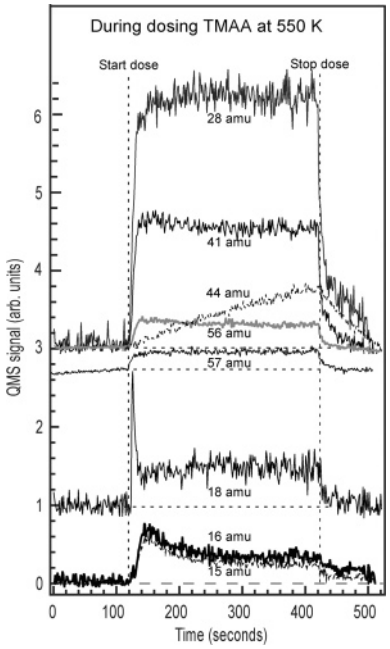

Figure 2. ISOMS measurements during the dosing of TMAA onto a clean annealed rutile TiO_2(110) surface at 550 K. Along the time axis, the dose started at 120 s and ended 300 s later at 420 s. Profiles have been adjusted for background effects and are offset for easier viewing.

Because it is particularly relevant during dosing at 550 K where a steady-state reaction occurred, we searched for detectable product evolution during dosing at 300 K. While briefly described in earlier work,[7] more detail is given here, since the superposition of photochemical and thermal reactions is evident in the photolysis experiments. Dosing the clean substrate was compared with dosing an inert flag held at 300 K and placed between the dosing tube and the sample. Among the nine signals compared—15, 16, 18, 28, 32, 41, 44, 56, and 57 amu—only 32 amu exhibits no measurable response when dosing. The others all increase when dosing begins, but after adjusting for the slightly different geometric positions of the flag and sample, only three signals—15, 16, and 57 amu—exhibit detectable differences (Figure 1). Differences in the 15 and 16 amu signals (upper panel) are small but at the outset are clearly larger when dosing the substrate. Both the 15 and 16 amu signals are attributed to CH_4. Differences in the 57 amu signal (lower panel) are more difficult to distinguish but are always higher when dosing the flag, as shown by the integral embedded in the lower panel. From these data, we conclude that, during dosing at 300 K, thermal reactions accompanied by the desorption of products are negligible, other than a transient of methane, the source of which is not known. Nearly all incident TMAA either scatters off TiO_2(110) or chemisorbs. This observation is relevant for photolysis at 300 K where ejected products are relatively intense.

Preparation at 550 K. Since TPD without photolysis after dosing at 300 K leads to relatively strong thermal desorption of products setting in just above 300 K, it was difficult to determine whether photolysis at, or below, 300 K produces chemisorbed intermediates that are relatively stable and react to form products above 300 K. Dosing at 550 K was one way to reproducibly prepare a surface that after cooling did not show any desorption below 500 K. Above 500 K, the TPD profiles after a 550 K TMAA dose are like those measured after dosing at 300 K, that is, dominated by CO, *i*-C_4H_8, and *i*-C_4H_{10} with peaks at 650 K. Both X-ray photoelectron spectroscopy (XPS) and TPD[7] results are consistent with the presence of TMA. On the basis of calibrated TPD spectra, the TMA coverage is 0.3 ML, half that achieved by saturation dosing at 300 K.[7]

Whereas product desorption during dosing at 300 K was minimal, steady reaction of incident TMAA to form products was easily observed in ISOMS at 550 K. Extending prior ISOMS measurements, Figure 2 shows background-subtracted profiles measured during dosing TMAA at 550 K. After collecting baseline data for 120 s, TMAA was introduced for 300 s. When dosing starts, several signals increase sharply, but the 44 amu signal is qualitatively different. After significant background correction (see below), it rises monotonically and with the same time dependence as when TMAA is dosed onto the flag. Thus, TMAA thermally decomposing on TiO_2(110) at 550 K produces little if any CO_2 and the observed increase is attributed to a steadily increasing background partial pressure. The steplike initial response of the other signals is taken as indicating thermal reactions of incident TMAA that produce CO (28 amu), H_2O (18 amu), *i*-C_4H_8 (56 amu), *i*-C_4H_{10}, and CH_4 (15 and 16 amu). (43 amu, not shown, is coincidentally superimposable on the 56 amu profile.) The sharp transient response of 18 amu is unique and is attributed to rapid formation and desorption of water during the accumulation of TMA (without desorption) to its steady-state value. It may also be related to the bridging oxygen atom vacancy concentration (see below). The 57 amu signal, attributed mainly to TMAA that scatters off the hot titania surface without reaction, becomes constant in a relatively short time (<20 s). Beyond 120 s, all the rates are constant. When dosing stops, all the signals, including the 44 amu signal, drop relatively slowly as the vacuum system relaxes. The absolute amounts, calculated using the areas beneath the profiles, are (in units of 10^{14} cm^{-2}) 2.2 for CO, 2.1 for H_2O, 1.3 for *i*-C_4H_8, and 0.3 for *i*-C_4H_{10}. The amount attributed to CH_4 is unknown. As described in detail in the Discussion section, the steady-state stoichiometric relations among the products are important.

Preparation at 100 K. Preparing samples by dosing and photolyzing at 100 K was motivated by differences and

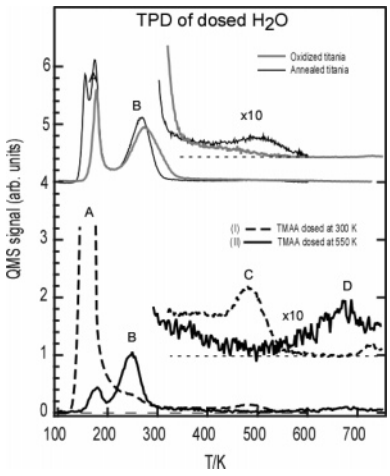

Figure 3. TPD of water dosed at 100 K onto four different surfaces—(I) TMA-covered TiO_2(110) prepared at 300 K, (II) TMA-covered TiO_2-(110) prepared at 550 K, annealed TiO_2(110), and oxidized TiO_2(110). Four desorption regions are identified along the temperature axis—(A) multilayer H_2O, (B) H_2O chemisorbed on exposed Ti^{4+} sites, (C) OH recombination reaction to form H_2O, and (D) H_2O from source other than dose of H_2O and speculatively attributed to subsurface H and O.

similarities in the TPD intensity distributions above 300 K compared to those for doses at 300 K. For large doses at 100 K, the TPD spectra comprise numerous dose-dependent local maxima. As for doses at 300 and 550 K, the 2 and 44 amu profiles are exceptional and exhibit no local maxima. The peak temperatures with proposed identification given in parentheses include the following: 190 K (multilayer TMAA), 235 K (undissociated TMAA in contact with Ti^{4+} surface cations), 450 K (TMAA), 480 K (water, CO, and TMAA), and 650 K (CO, *i*-butene, and *i*-butane with minor amounts of other species). Compared to doses at 300 K, the spectra above 500 K are very similar, but between 300 and 550 K, significantly less material desorbs. The calculated sum of TMAA and C_4 products (*i*-butene + *i*-butane) desorbing above 300 K is 1.1×10^{14} cm^{-2} (0.21 ML), 3-fold smaller than that for saturation doses at 300 K.

For low doses, $\leq$0.1 ML, the only species desorbing below 500 K is H_2O, with local maxima at 325 and 500 K, much of which is attributed to uptake from background. All the other maxima are located at 650 K. The 28, 41, 43, 56, and 57 amu profiles are prominent and proved to be most useful in diagnosing the thermal chemistry. Motivated to search for stable intermediates formed during photolysis, we photolyzed a submonolayer (1.3×10^{13} cm^{-2}, 0.03 ML) dosed at 100 K.

It is also important to note that, in TPD after saturation at 300 K, the coverages determined (0.6 ML) are 3-fold higher than the maximum desorbing above 300 K for multilayer doses at 100 K (0.21 ML). This result indicates that important thermal chemistry occurs during dosing at 300 K that does not occur either during dosing at 100 K or during subsequent TPD. While there is evidence for some deprotonation during adsorption at 100 K, we speculate that surface diffusion of TMAA is inhibited at 100 K and that the highly ordered (1×2) TMA arrays, imaged in STM following doses at 300 K, do not form readily.

Probing Surfaces with H_2O. As one sensitive test of the as-prepared surfaces, we dosed H_2O at 100 K and measured the TPD spectra (Figure 3).[8] Four regions are labeled where differences appear depending on how the surface was prepared. For the two cases of central interest here, H_2O dosed after exposure of annealed TiO_2(110) to TMAA at either 300 (I, dashed line) or 550 K (II, thick line), there are easily recognized differences. Compared to I, the intensity of II is weaker in region A and the onset *T* is higher, is stronger in region B, is weaker (negligible) in region C, and is stronger in region D. For comparison, TPDs of water dosed on annealed TiO_2(110) and on oxidized TiO_2(110) are included in Figure 3. In region C, there is a peak for the annealed surface but not the oxidized surface. Region B intensities are comparable, and the differences in region A are attributable to differences in dosing and the unsaturable character of this TPD region. There is no intensity in region D for either the annealed or oxidized surface.

Regardless of the H_2O dose, even submonolayer amounts, on a surface prepared by dosing TMAA at 300 K, the TPD onset of 18 amu is located at 135 K in region A. This onset is typical of thick multilayers, that is, bulk H_2O. For the other surfaces, the onset is shifted into region B. This reflects monolayer wetting of surfaces with exposed Ti^{4+} followed by preferential layer-by-layer growth for a few subsequent layers. Thus, as the coverage of H_2O increases, there is a slow downward shift of the onset temperature toward 135 K. Region B is attributed to undissociated H_2O desorbing from exposed Ti^{4+}. This peak is strong in three of four cases. It is suppressed only for H_2O dosed on a surface after saturation with TMA at 300 K. Evidently, there are Ti^{4+} sites readily available for chemisorption of H_2O when the TMA coverage is 0.3 ML (550 K dose) but not 0.6 ML (300 K dose).

The H_2O that desorbs between 450 and 500 K, region C, is attributed to disproportionation of OH groups arranged along the bridging oxygen atom rows. It is clearly present for H_2O dosed on TiO_2(110) after annealing to 850 K and has been used as a measure of the number of bridging oxygen atom vacancies.[14] This peak is absent for H_2O dosed on oxidized TiO_2-(110), indicating that exposing annealed TiO_2(110) to O_2 fills vacancies, a conclusion confirmed by STM measurements.[9,11] Critical for the experiments reported here, the 450 K peak is also absent when H_2O is dosed after dosing TMAA at 550 K. Evidently, exposure to TMAA at 550 K involves the formation of surface species that block (perhaps fill) the bridging oxygen atom vacancies. The relatively strong H_2O peak in region C after dosing TMAA at 300 K is consistent with deprotonation of TMAA to form OH at bridging oxygen atoms. The disproportionation of these removes bridging O atoms that are subsequently replaced when TMA decomposes at 650 K.

Only two (I and II) of the 18 amu profiles in Figure 3 exhibit intensity in region D. Both involve TMAA, but not H_2O, dosing. This high-temperature H_2O desorption overlaps but peaks 20—40 K higher than the collection of other profiles that peak at 650 K (Figure 4). Furthermore, the intensity is 10 times larger for the dose at 550 K as compared to that at 300 K. Evidently, there is a temperature-dependent process involving species derived from TMA that lead to this high-temperature H_2O peak

State of Surface after TPD. For all preparations described above and after all photolysis experiments, TPD to 800 K left a surface devoid of carbon based on Auger electron spectroscopy (AES) and XPS.[7] Furthermore, any bridging oxygen atoms that were removed by OH disproportionation during dosing, photolysis, or heating were replaced, since, when H_2O was dosed after annealing to 850 K in a vacuum, the experiment-to-experiment variation in the amount of H_2O dissociated was minimal.

4. Photolysis Results

4.1. Temperature Programmed Desorption. *Photolysis at 100 K after Saturation Dose of TMAA at 300 K.* There are easily recognized differences in TPD with and without photolysis at 100 K of TMAA dosed to saturation at 300 K. Figure 4

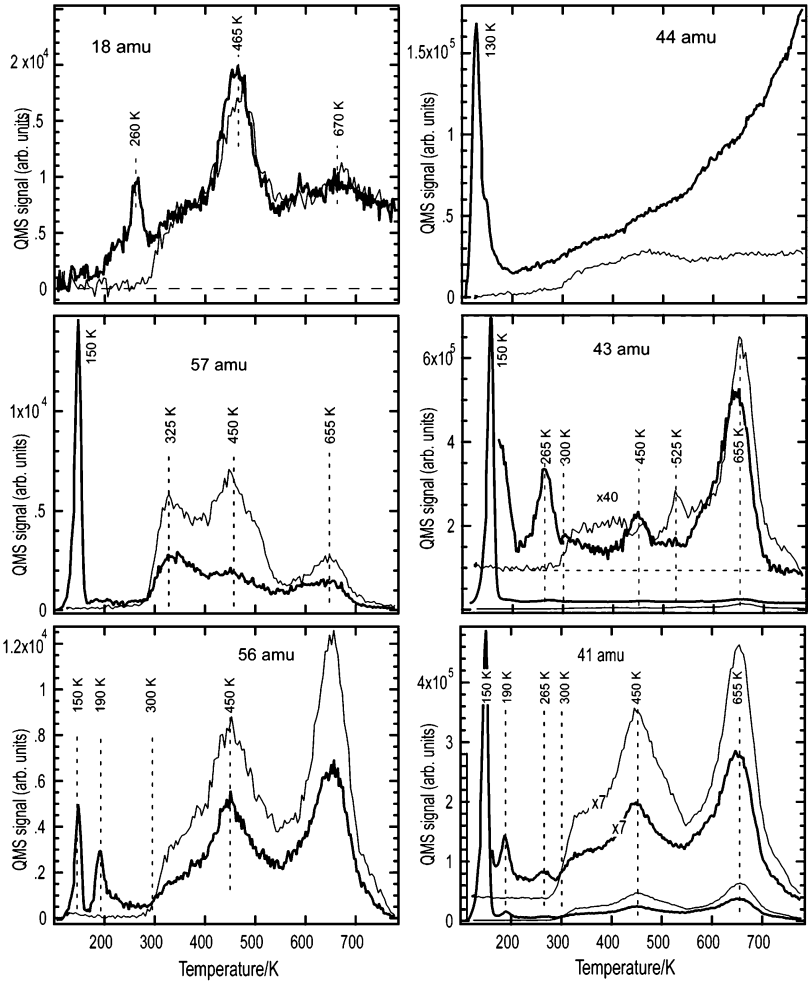

Figure 4. TPD spectra (thick lines) following 50 min of UV photolysis at 100 K of a TMA-saturated TiO_2(110) surface prepared by dosing TMAA at 300 K. To minimize the temperature rise during photolysis, the light source was mechanically chopped (16% duty cycle). The temperature increase was no more than 5 K during the 50 min irradiation. For comparison, TPD spectra for the same dose but without photolysis (thin lines) are shown. Each panel has a different scale on the vertical axis. The 28 amu signal was not collected in this set of experiments.

illustrates for photolysis with the chopped source at 100 K. Each of the six panels has a different intensity scale. The six ions—18, 41, 43, 44, 56, and 57 amu—were selected on the basis of numerous thermal and photochemical experiments that identify H_2O, CO_2, *i*-C_4H_8, *i*-C_4H_{10}, and TMAA as major contributors to the TPD spectra. Carbon monoxide, another major TPD product monitored by 28 amu, was not followed in these experiments because the background pressure of CO in the chamber was relatively high and fluctuated. In other experiments, with or without photolysis, there is unambiguous evidence for CO forming and desorbing at high temperatures in TPD but no evidence for its formation during photolysis. In Figure 4, the thick lines were measured with, and the thin lines without, photolysis. The initial TMA coverage is 0. 6 ML (3×10^{14} cm^{-2}), that is, slightly more than 1 TMA for each pair of exposed Ti^{4+} cations. In each case, constant backgrounds were subtracted to zero the intensities at 100 K. The 18 amu signal monitors the amount of H_2O present. The two spectra differ mainly below 300 K where, after photolysis, there is increased intensity and a peak at 260 K. Above 300 K, the integrated intensity differs by no more than 5%.

The 44 amu profiles exhibit major differences. Before photolysis, there are relatively weak, local maxima on an otherwise rising background. The weak maxima are accounted for as fragmentation of TMAA (due to $C_3H_8^+$ and/or $C_2H_4O^+$ fragments). After photolysis, the peak at 130 K is fully accounted for as CO_2 desorbing from the substrate,[17] while the steeply rising unstructured signal above 500 K is attributed to thermal desorption of CO_2 from slowly warming surfaces other than TiO_2(110). The identification of the 130 K peak as CO_2 is based on the fact that the peak position and shape, including the shoulder, match the 44 amu TPD profiles for CO_2 directly dosed at 100 K. For lengthy photolyses as in Figure 4, further analysis shows that some, but by no means all, of the 44 amu signal at 130 K is the result of background flux of CO_2. Some of the background CO_2 is the result of scattered ultraviolet photons inducing desorption of CO_2 from those vacuum system surfaces with $T > 130$ K. Supporting evidence is provided below (Figure 11); when the substrate is rotated to avoid direct interception of the incident photons, there is a prompt rise of the 44 amu signal when the light source is turned on.

The four other panels—41, 43, 56, and 57 amu—taken together, provide evidence for identifying products, in addition to H_2O and CO_2, that are formed during thermal and photochemical processing. The 43 amu profile is dominated by *i*-C_4H_{10} and the 56 amu profile by *i*-C_4H_8. The 57 amu profile below 550 K, but not above, is dominated by TMAA. As noted earlier, the 41 amu profile, assigned to $C_3H_5^+$, is useful because it is an intense, easily detected fragment of *i*-C_4H_8, *i*-C_4H_{10}, and TMAA, the major species identified in TPD. In Figure 4, there are five 41 amu peaks after photolysis—150, 190, 265, 450, and 655 K. Of these, only two—450 and 655 K—are present without photolysis (thin line). There is also a prominent shoulder in the region between 300 and 400 K before and after irradiation.

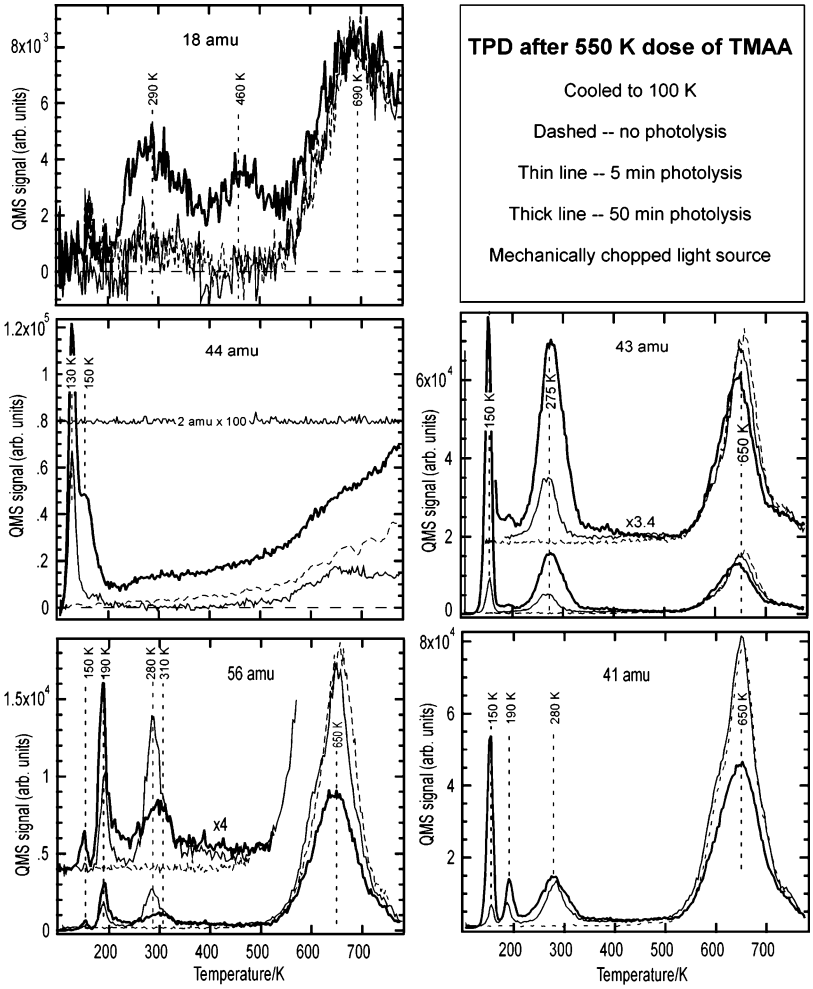

Figure 5. TPD spectra collected after dosing TMAA onto clean TiO_2(110) at 550 K and reducing the temperature below 120 K (dashed lines) and after photolysis at 100 K with a chopped (16% duty cycle) light source for 5 (thin lines) and 50 min (thick lines). A profile for 2 amu, scaled by 100 times, is inserted in the 44 amu panel. Note that each of the panels has a different *y*-axis scale.

In separate experiments, we established that the integrated (time domain) 41 amu intensity above 300 K generally provides a semiquantitative estimate of the relative amount of TMA on the surface before and after photolysis. This estimate has proven adequate except under conditions where more than 50% of the initial coverage is photolyzed. Even though a number of different thermal processes occur during TPD and even though several products desorb, all of the identified C_4- and C_5-containing products have fragmentation patterns with significant 41 amu contributions. From Figure 4, the ratio of integrated 41 intensities with and without photolysis is 0.55; that is, 45% of the initial TMA coverage was converted to products during this photolysis. Similar analysis, applied in another experiment to the 28 amu intensity, gives the same conclusion.

Turning to the low-temperature portion of the 41 amu profile, the lowest temperature peak after photolysis occurs at 150 K and is accompanied by peaks in 43, 56, and 57 amu. When *i*-butane (*i*-C_4H_{10}) is directly dosed onto clean TiO_2(110), it adsorbs molecularly and, up to monolayer coverage, desorbs at 150 K with the fragmentation pattern observed at 150 K in Figure 4. The peak at 190 K in 41 amu is accompanied by a 56 amu peak but no peaks in 43 or 57 amu. Both the peak position and fragmentation pattern match those found when *i*-butene (*i*-C_4H_8) is dosed directly; like *i*-butane, the adsorption is nondissociative and up to monolayer coverage peaks at 190 K. Moving to higher temperature, there is a relatively weak 41 amu peak at 265 K that is accompanied by a weak 43 amu peak and no detectable 56 or 57 amu peak. The fragmentation pattern is consistent with the desorption of *i*-butane; the predicted 56 and 57 amu signals are below detectability. Thus, we assign the peaks at 150 and 265 K to *i*-butane and that at 190 K to *i*-butene. Between 100 and 300 K, there is no evidence for desorption of TMAA.

In the region between 300 and 750 K, an earlier report,[7] describing thermal reactions of TMA that occur during TPD, ascribed the 57 amu signal to TMAA desorption. A more detailed analysis, based on the 57 and 59 amu signals, shows that between 300 and 550 K, but not above 550 K, the I_{59}/I_{57} intensity ratio is consistent with TMAA (not shown). Above 550 K, there is excess 57 amu intensity, and that excess is tentatively assigned to 2,2,3,3-tetramethyl butane, a species that has a relatively strong 57 amu fragmentation component and is the result of C−C bonding of two *tert*-butyl groups.

Analysis of other profiles between 27 and 90 amu (not shown) provides evidence for the desorption of small amounts of CH_4 and/or CH_3 accompanied by small amounts (<5% of the sum of TMAA + *i*-butane + *i*-butene) of other C_4 and C_5 molecules between 550 and 780 K, all peaking within 10 K of 650 K. These include methyl isopropenyl ketone ($CH_3CH(CH_2)C(=O)CH_3$) that accounts for small peaks in the 84 and 69 amu profiles. Another species, 3-methyl-2-butanone ($(CH_3)_2CHC(=O)CH_3$), accounts for weak 71 and 86 amu peaks. A third species, 2-methyl-1,3 butadiene ($CH_2(CH_3)CCHCH_2$), accounts for 67 and 68 amu peaks. In TPD after photolysis, we assume

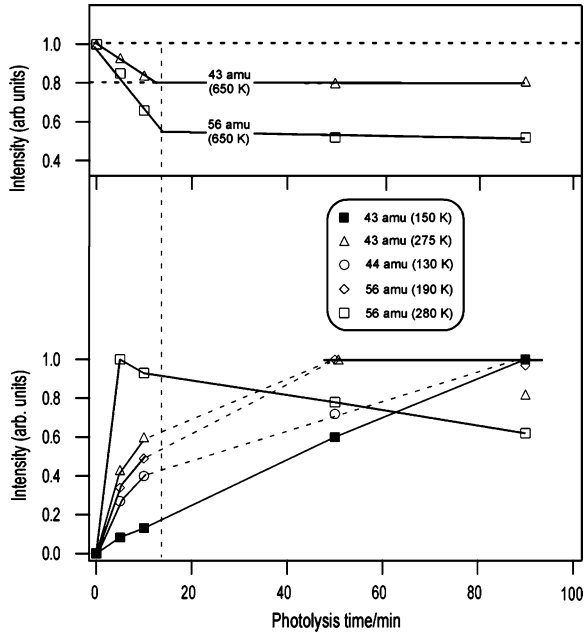

Figure 6. From profiles of Figure 5 and other experiments involving the photolysis of a surface prepared by dosing TMAA at 550 K, the TPD peak areas after photolysis at 100 K (chopped sources with 16% duty cycle). Each curve is identified with a mass and a peak temperature. The upper panel shows consumption of the 43 and 56 amu profiles associated with thermal decomposition of TMA. The lower panel shows the growth and subsequent decay or saturation of TPD peaks appearing below 300 K and showing the accumulation of photolysis products.

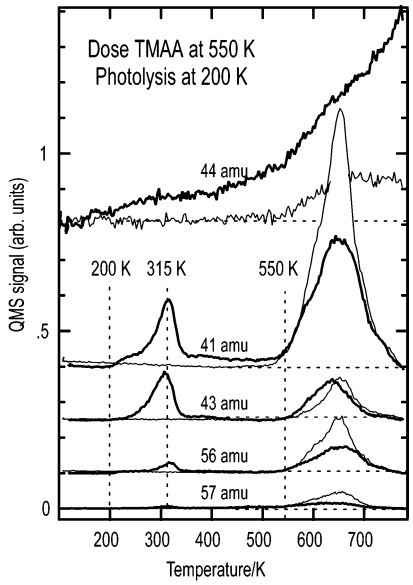

Figure 7. TPD with (thick lines) and without (thin lines) photolysis at 200 K of a surface prepared by dosing TMAA at 550 K.

that these products are also formed and desorb. In passing, it is noteworthy that each of these molecules contributes to the 41 amu intensity profile that we used, as described above, to monitor the relative amount of TMA species present before or after photolysis. After TPD to 750 K, the surface is free of carbon based on AES.

Returning to a description of Figure 4, notice that above 300 K the 56 amu signal has the same shape but the intensity is half that measured without photolysis. In this same region, there are significant changes in the distributions of 43 and 57 intensity. After making adjustments for fragmentation, these profiles were converted to estimates of the absolute amounts of TMAA, i-C_4H_8, and i-C_4H_{10} that desorb in two separate regions—above and below 300 K (Table 1). The intensities below 300 K are taken as measuring the *i*-butene and *i*-butane formed during photolysis, and those above 300 K, the amount of TMA remaining after photolysis. The noteworthy points to make are the following: (1) The sum of i-C_4H_8 and i-C_4H_{10} desorbing after photolysis equals, to within 10%, the total without photolysis; that is, there is no evidence for C_4 and C_5 product ejection during photolysis at 100 K. (2) According to this table, 48% of the initial TMA is consumed (compare the "total" values for before and after photolysis), a value comparing favorably with that (45%) based on the integrated 41 amu signals described above. (3) Above 300 K, the fractional decreases of *i*-butene and TMAA exceed that of *i*-butane.

TABLE 1: Desorbed Amounts before and after Photolysis

species	no photolysis (molecules/cm^2)	photolysis: amount desorbing above 300 K (molecules/cm^2)	photolysis: amount desorbing below 300 K (molecules/cm^2)
TMAA	1.26E+14[a]	4.95E+13	0
i-C_4H_8	1.49E+14	8.85E+13	6.86E+12
i-C_4H_{10}	1.56E+13	1.35E+13	1.59E+14
total	2.90E+14	1.52E+14	1.66E+14

[a] Uncertainties are roughly 20% for each numerical value.

Photolysis at 100 K after 550 K Dose of TMAA. Photolyzing for various times at 100 K with the chopped source after dosing at 550 K, rather than 300 K, was helpful in identifying the desorption of photolysis products around 300 K. Figure 5 summarizes in five panels TPD results for three TPD experiments—photolysis for 0, 5, and 50 min—after dosing at 550 K. While not measured in these photolysis experiments, other experiments show that the 57 amu profiles contribute no more at 650 K than in Figure 4.

Using the 41 amu intensity as a monitor, the initial coverage of TMA is 50 ± 5% (1.6×10^{14} cm^{-2}) of that for dosing at 300 K (3.1×10^{14} cm^{-2}). This agrees with relative coverages based on XPS and independent TPD measurements.[7] To account for background variations, the 18 amu plots shown were obtained by subtracting a different constant signal from each of them to force both plots to zero at 100 K. Compared to TPD without photolysis (dashed line), the 18 amu profile after 5 min of photolysis (thin line) is indistinguishable but after 50 min of photolysis (thick line) the intensity increases across the region from 200 to 550 K, but not around the 690 K peak. The absence of a detectable increase for the 5 min photolysis is relevant in comparison to relatively strong increases in other product signals attributable to photolysis and, more importantly, to the observation noted below that the rate of product formation is highest in the first minutes of photolysis. Most of the H_2O increase for the 50 min photolysis originates from background adsorption of H_2O. However, the situation is more complex. The emergence of an 18 amu peak at 460 K is evidence for OH recombination among OH species located along bridging O atom rows of TiO_2-(110).[14] These form from background uptake of H_2O only if there are bridging oxygen atom vacancies available. These were not available when water was dosed on the surface prepared by dosing TMAA at 550 K (Figure 3), suggesting that photolysis leads to their availability.

The 44 amu (CO_2) profiles are positioned and distributed as in the photolysis after a 300 K dose; there is a strong peak at 130 K with a shoulder toward higher temperature. As discussed above, a significant fraction of this CO_2 signal is due to adsorption from background, not photolysis of TMA. In this experiment, we confirmed, by tracking the 2 amu signal (plotted

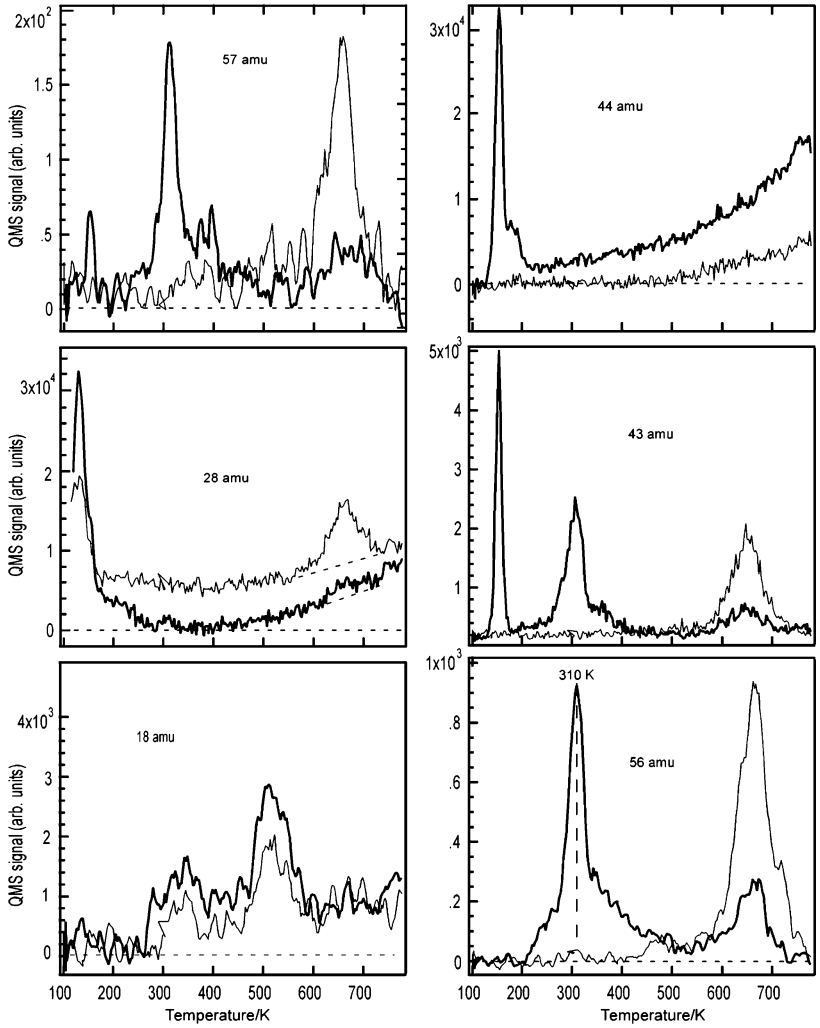

Figure 8. TPD with (thick lines) and without (thin lines) photolysis of submonolayer TMAA dosed and photolyzed at 100 K. Each panel has a different scale for the quadrupole mass spectrometer (QMS) signal.

within the 44 amu panel), the common observation that negligible H_2 is found in TPD for TMAA-dosed TiO_2(110) that is activated either thermally or photochemically.

In the other three panels, there are interesting similarities and differences (compared to Figure 4 for TMAA dosed at 300 K) in the product distributions, most notably in the temperature region near 300 K. Consider the 41 amu profiles. As for photolysis after a 300 K dose of TMAA, there are three peaks below 300 K—150, 190, and 260 K—for photolysis after a 550 K dose. The 43 amu profiles for the two dosing conditions are comparable; there are strong peaks at 150 and 270 ± 5 K. In the 56 amu profiles, there are peaks at 190 and 150 K for both dosing conditions, but the distributions differ. For 50 min photolyses, the 56 amu profiles differ significantly; there is significant intensity in the 300 K region when TMAA is dosed at 550 K. Compared to the signal in the absence of photolysis (dashed line in Figure 5), the 56 amu intensity profile after photolysis is somewhat more intense across the whole region between 300 and 550 K. It is impossible to determine whether a similar broad increase occurs for photolysis after a 300 K dose of TMAA (Figure 4).

For a TMA-covered surface prepared by dosing at 550 K, the variation of the peak areas with photolysis time (Figure 6) provides insight. At some time between 10 and 50 min, the 43 and 56 amu intensities at 650 K become nearly constant at 80 and 50% of their initial values, respectively (upper panel). Similarly, the 41 amu intensity stabilizes at 60% of its initial value (not shown). As described in the Experimental Section, a recently installed light fiber optic brings all the incident radiation directly onto the surface, thereby minimizing the effects of stray radiation. At comparable incident intensity, experiments with the fiber in place (not shown) indicate that between 12 and 30 min the 56 and 43 amu intensities at 650 K each drop by no more than 5%. Taking this into account, the curves in the upper panel of Figure 6 are constructed from two linear segments, one through the short time and the other through the long time data. In view of the rate quenching evident in Figures 9—11 (see below), describing the early time results as linear is clearly an oversimplified approximation but does provide a reasonable estimate of the time required (15 min) for the 43 and 56 amu intensities to become constant (vertical dashed line in Figure 6).

For products that desorb below 550 K after photolysis, the lower panel of Figure 6 plots normalized peak areas, as a function of photolysis time, for individual product peaks identified in Figure 5. The 44 amu peak at 130 K is assigned to CO_2; its intensity (circles) increases sharply in the first 10 min, mirroring the decay of the 43 and 56 amu profiles in the upper panel. Beyond 10 min, the linear increase is shown as a dashed line because no more than 15% of the increase is attributable to photolysis. The remainder is ascribed to accumulation from background intensity. Consistent with this assignment, absolute coverage estimates, calculated as for Table 1, show that between 10 and 90 min neither the small (nearly negligible) decreases

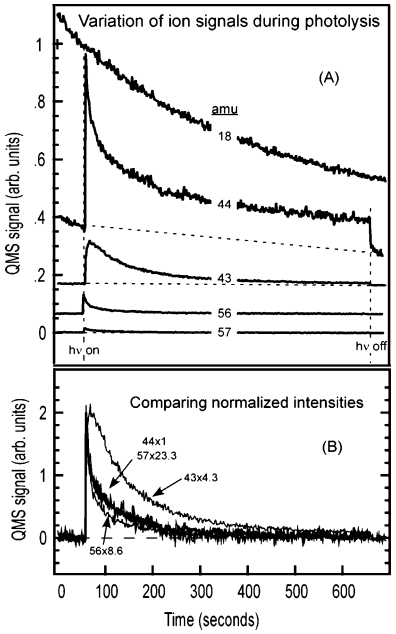

Figure 9. ISOMS data gathered during photolysis at 300 K of a surface saturated with TMA by dosing at 300 K. In the upper panel, curves are offset for clarity. Along the time axis, the photolysis began at 60 s and ended 600 s later at 660 s. In the lower panel, the 43, 44, 56, and 57 amu profiles normalized to the 44 amu maximum are shown to demonstrate the slower decay of the 43 amu signal and the faster decay of the 56 amu signal.

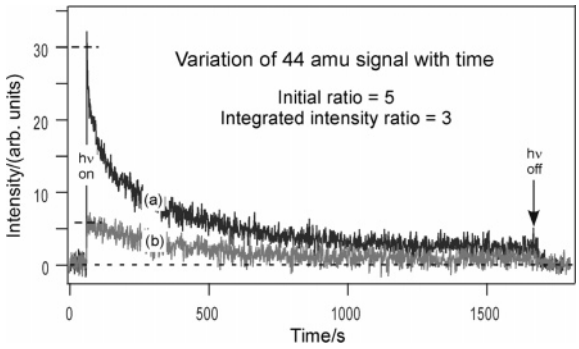

Figure 10. Comparison of the ISOMS 44 amu profiles during photolysis at 300 K of TMA-covered rutile TiO_2(110) surfaces prepared by dosing TMAA at (a) 300 K and (b) 550 K.

of the 43, 56, and 57 amu intensities at 650 K nor the increased 43 amu intensity at 150 K can account for the increased 44 amu intensity. The 43 amu peak at 275 K is assigned to *i*-butane. It rises together with the others and then, although the uncertainty is rather large, appears to decay between 50 and 90 min of photolysis.

The 43 amu intensity at 150 K (filled squares) is ascribed to *i*-butane. It grows linearly with photolysis time from 5 to 90 min. Beyond 10 min, the growth is attributed, as detailed in the Discussion section, to the photolysis of adsorbed species formed earlier in the process that led, in TPD, to the 56 amu signal at 280 K. The 56 amu peak at 280 K (open squares), assigned to *i*-butene, reaches its maximum in the first 5 min of photolysis and then decays monotonically and approximately linearly between 5 and 90 min. The 56 amu peak intensity at 190 K (diamonds), also assigned to *i*-butene, rises nonlinearly to 50 min and then remains constant between 50 and 90 min.

Photolysis at 200 K after 550 K Dose of TMAA. To test the hypothesis that photolysis at 100 K, not subsequent heating, leads to adsorbed species giving rise to the C_4 molecules

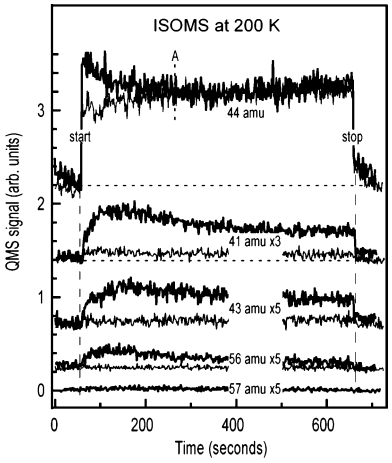

Figure 11. ISOMS data for photolysis at 200 K after dosing TMAA onto clean TiO_2(110) at 550 K. Thick lines are the response to photons of TMA-covered substrate and the chamber. Thin lines are the background response of the chamber to UV irradiation (substrate turned away from incident light). Irradiation started at 60 s and stopped at 660 s. Linear baselines have been subtracted from each curve to force a zero at the start and finish of the profiles. Pairs of curves are offset for easier viewing.

desorbing between 200 and 350 K in subsequent TPD, TMA prepared by dosing at 550 K was photolyzed (unchopped) for 10 min at 200 K, high enough to release CO_2 and physisorbed *i*-C_4H_8 and *i*-C_4H_{10} but not the proposed chemisorbed C_4 intermediates responsible for the TPD peaks between 250 and 300 K. After photolysis, the temperature was lowered to 100 K for TPD (Figure 7). The 41 amu TPD intensity above 450 K decreases by 32%, indicating the extent of photolysis, and a new intensity appears between 200 and 350 K with a peak at 315 K. When the same dose was photolyzed at 300 K, the 41 amu signal decrease was comparable (36%). The CO_2 profiles before and after photolysis are monotonically rising and are attributed to desorption from liquid nitrogen cooled nonsample surfaces that warm slowly and release CO_2 accumulated from the background before and during photolysis.

The results of Figure 7 are consistent with photolysis at 200 K to form physisorbed CO_2 and chemisorbed C_4 species. The CO_2 desorbs (direct evidence provided below), while at least some of the C_4 species are retained, leading to the TPD peaks at 315 K. The 43 amu peak desorption temperature (315 K) is 40 K higher in Figure 7 than in Figure 5. While it remains to be determined what structural and kinetic factors lead to this difference, thermally activated kinetics superimposed on the nonthermal photochemistry must be considered. Regarding this question, the following observations are relevant. For TMAA dosed at 550 K, photolysis at 200 and 100 K for equal times with the unchopped light source leads to the same amount photolyzed, while that at 300 K was measurably larger. Further evidence regarding thermal chemistry during photolysis comes from the ISOMS results described below.

Photolysis at 100 K after Dose at 100 K. In one interesting experiment, we dosed and photolyzed, both at 100 K, submonolayer TMAA (0.02 ML $= 1.1 \times 10^{13}$ TMAA cm^{-2}) with the chopped light source (20 min) (Figure 8). The 28 amu profile was recorded in this case. If this submonolayer dose is not exposed to UV photons (thin lines), the 28, 43, 56, and 57 amu profiles do not rise below 550 K but all peak sharply at 650 K. There is no peak in 44 amu, and there are two peaks in 18 amu—350 and 500 K. After photolysis for 20 min, the high-temperature 28 amu peak is barely above background, while the high-temperature 43, 56, and 57 amu peaks are strongly

suppressed. As for photolysis after 550 and 300 K doses, that is, 0.3 and 0.6 ML of TMA, there are relatively strong peaks at 310 K in 43, 56, and 57 amu, each with a broad shoulder extending from 350 to 500 K. There are strong peaks at 155 K in the 44 and 43 amu profiles, but the shoulder at 175 K in the 44 amu profile is absent in the 43 amu spectrum. After photolysis, there is enhanced intensity at 120 K in the 28 amu profile but no new low-temperature features. Interestingly, for this or multilayer doses at 100 K, there is no clear evidence for an 18 amu peak between 650 and 700 K that is typical for larger TMAA doses at 300 and 550 K (Figures 3−5).

For the same number of incident photons, it is interesting to compare estimates of the fraction of the initial coverage (and number/cm^2) of adsorbate species converted to products. For the above experiment, 80% (8.8×10^{12} cm^{-2}) of the initial coverage was photolyzed. For the surface prepared by dosing at 550 K, 60% (9.6×10^{13} cm^{-2}) was photolyzed, and for a saturation dose at 300 K, 45% (1.4×10^{14} cm^{-2}) was photolyzed.

4.2. Isothermal Mass Spectrometry (ISOMS). *Photolysis at 300 K after 300 K Saturation Dose of TMAA.* Direct evidence for product ejection during irradiation was obtained by ISOMS, that is, monitoring the gas phase by mass spectrometry during irradiation. For a surface saturated and photolyzed (without chopping) at 300 K (Figure 9), the prompt response followed by strong decay is characteristic. Of the five profiles shown, the 18 and 43 amu curves have a different structure than the other three. There is a negligible response in the 18 amu profile when the photons are turned on or off. The steady decay of the 18 amu signal is attributed to the slowly decaying background signal after the substrate is annealed to 850 K before dosing. The 43 amu signal responds promptly but then continues to increase for 10−12 s before it maximizes and begins to decay. The other profiles—44, 56, and 57 amu—all maximize within the first cycle (1.6 s) of the mass spectrometer data gathering program and then decay much more sharply than the decay of the surface TMA coverage. When the photolysis ends, there are detectable drops in these signals. For the 44 amu profiles, blank photolysis experiments show that nearly all the ending response (>200 s) and a significant fraction of the beginning response is the result of CO_2 arising from UV photons striking surfaces other than TiO_2. While there are background signals at 56 and 57 amu, these are not altered significantly by introducing UV light.

To compare the time dependence of these signals in more detail, Figure 9 replots these data after background subtraction and normalization at the maximum values. The decays of the 44 and 57 profiles are indistinguishable. Compared to these two, the 43 amu profile decays more slowly and the 56 profile slightly more rapidly. The slower decay of the 43 amu (*i*-butane) profile may be related to the slow growth of the 150 K *i*-butane intensity in the 100 K photolyses.

To within a factor of 2, 10^{17} photons/cm^2•s is the flux to the surface of photons with energies exceeding the band gap (3.2 eV) of TiO_2. The estimated average i-$C_4H_8 + i$-C_4H_{10} production rate over the first 10 s of photolysis (Figure 9) is $(1.5 \pm 0.3) \times 10^{12}$ molecules/cm^2•s, calculated using sensitivity factors derived from directly dosed i-C_4H_8 and i-C_4H_{10} and assuming 1 ML is $(3.5 \pm 0.3) \times 10^{14}$ molecules/cm^2 for each. The ratio provides an estimate of 1.5×10^{-5} molecules per incident photon. This yield estimate, while crude, underscores the following point: conversion of the incident photon flux to products on TiO_2-(110) is very inefficient.

Photolysis at 300 K after 550 K Dose of TMAA. When TMAA was dosed at 550 K and photolyzed at 300 K, the rate of product ejection was lower than that for doses at 300 K and was more than accounted for by the difference in initial coverage. Figure 10 illustrates for CO_2 ejection measured using the optical fiber photon delivery system where the CO_2 background correction is relatively small. While the initial coverages differ by a factor of 2, the *initial* photolysis rate differs by a factor 5; that is, the specific initial rate (rate per TMA) is lower by a factor of 2.5. The rate difference decreases rapidly with time, and beyond 1000 s, the ratio does not exceed 2. Overall, the ratio of the integrated signals is larger by a factor of 3 for the dose at 300 K. Ejection of CO_2 is a measure of decarboxylation and can be compared to the approximation described earlier that is based on the 41 amu TPD intensity; the integrated ejected 41 amu intensity is a factor of 3.5 larger for photolysis of the 300 K dose. On the basis of the TPD peak areas of the 41 and 28 amu signals, (55 ± 3)% (0.33 ML) of the initial coverage (0.6 ML) remains after irradiating the 300 K dose and (40 ± 3)% (0.12 ML) of the initial coverage (0.3 ML) remains after irradiating the 550 K dose.

Photolysis at 200 K after 550 K Dose of TMAA. After a dose at 550 K, product desorption during photolysis at 200 K (not using the optical fiber) was also observable (Figure 11). The temperature rose from 193 to 205 K during the photolysis. The thin lines reflect the background response to photons, while the thick lines represent the response of the TMA-covered substrate plus the background. When photons are introduced, the 44 amu profile rises promptly to its maximum, as in Figures 9 and 10, but the 41, 43, and 56 amu maxima are delayed, by 60 s for 56 amu and by 100 s for 41 and 43 amu. The 57 amu profile exhibits no detectable response to photons. While the response of the chamber to irradiation (thin line) is relatively large for 44 amu, there is clearly an additional response when the TMA-covered substrate is irradiated (thick line). For 44 amu, the difference between the thick and thin lines decays quickly with time and the two curves become indistinguishable at point A located 200 s after the start and, from this point onward, the ejection of CO_2 is not discernible. The 41, 43, and 56 amu ejection rates from the TMA-covered substrate remain above the background throughout the 600 s irradiation period. Recall that, from TPD (Figure 7), 70% (0.21 ML) of the initial coverage (0.3 ML) remains after photolysis.

5. Discussion

The following discussion is subdivided, somewhat arbitrarily, into two subsections: Adsorption and Deprotonation and Photon-Driven Chemistry and Superimposed Thermal Chemistry. Scheme 1 illustrates several features of the system. The lower portion (A) depicts the TMAA molecule and the TiO_2-(110) surface. The three CH_3 groups of TMAA are depicted as single circles slightly larger than a carbon atom. All orientations of the incident TMAA molecules are assumed, and two are shown. For chemisorption and deprotonation, I is poorly oriented and II is favorably oriented. The TiO_2(110) surface comprises rows of Ti^{4+} cations and bridging O^{2-} anions. A bridging oxygen atom vacancy is indicated in the last row on the right-hand side. Both 6- and 5-coordinate Ti^{4+} cations are indicated, the latter exposed to the incident TMAA. The separation between the atoms in a given row is 0.298 nm, and the separation between the rows is 0.64 nm. The bridging oxygens are electron-rich and basic, while the 5-coordinate Ti^{4+} cations are electron deficient and acidic. The TMAA reacts with this surface by acid−base chemistry: the acid proton of TMAA

forms a bond with a bridging oxygen anion, and the acidic Ti^{4+} reacts with the basic carboxylate portion of TMAA. The result is depicted in panel B of Scheme 1. A more detailed description is provided in the following paragraphs. Photolysis of B leads to the ISOMS and TPD results presented above.

Adsorption and Deprotonation. Using the subscripts g, a, and p to denote gas, chemisorbed, and physisorbed species, the adsorption of TMAA can be represented using a sequence of phenomenological processes—adsorption to a physisorbed molecular precursor state (1_f), desorption (1_r), nondissociative chemisorption (2), and deprotonation to form bidentate (3) or monodentate (4) trimethyl acetate. Using tBu to denote $(CH_3)_3C$, the tertiary butyl portion of TMAA, the reactions are written as

$$tBuCOOH_{(g)} \rightleftarrows tBuCOOH_{(p)f} \text{ and } 1_r \quad (1)$$

$$tBuCOOH_{(p)} \rightarrow tBuCOOH_{(a)} \quad (2)$$

$$tBuCOOH_{(a)} + 2Ti^{4+} + (-O^{2-}-) \rightarrow (tBuCOO^{-})-(Ti^{4+})_2 + (-OH^{-}-) \quad (3)$$

$$tBuCOOH_{(a)} + Ti^{4+} + (-O^{2-}-) \rightarrow (tBuCOO^{-})-(Ti^{4+}) + (-OH^{-}-) \quad (4)$$

where Ti^{4+} is an exposed cation and $-O^{2-}-$ designates a bridging oxygen anion bound between a pair of Ti^{4+} cations lying beneath the surface plane. The chemisorbed $tBuCOOH_{(a)}$ is included to account for TMAA that desorbs between 300 and 400 K after dosing TMAA at 300 K (Figure 4). $(tBuCOO^{-})-(Ti^{4+})_x$ denotes, for $x = 1$ and 2, monodentate and bidentate trimethyl acetate.

We assume that bidentate TMA dominates the highly ordered (1×2) structures imaged in STM.[9-11] For a perfect TiO_2(110) surface and bidentate TMA, the predicted saturation coverage would be 0.5 ML, that is, 0.50 TMA/Ti^{4+}. On the basis of calibrated TPD, the saturation coverage formed during 300 K dosing is slightly higher (0.6 ML) and may involve some monodentate TMA or chemisorbed TMAA, the latter accounting for much of the TMAA that desorbs just above 300 K. As indicated in Figure 3 and described in detail elsewhere, the surface formed by saturation at 300 K is exceptionally hydrophobic.[8]

When dosing is carried out at 300 K, both the incident TMAA and the TiO_2(110) substrate are at the same temperature, so thermal accommodation is not an issue except for the three center-of-mass coordinates that bring TMAA into collision with the substrate. At this substrate temperature, the highly ordered (1×2) arrays[9-11] of TMA indicate that either TMA is mobile or, more likely, since STM images are stable when single TMA species are photochemically removed, the incident TMAA adsorbs in a weakly held precursor state, reaction 1_f, that lives long enough before desorbing (1_r) to sample many sites on the surface and deprotonate preferentially adjacent to previously formed TMA. The geometric arrangement used for dosing requires the collision of at least 80% of the inbound TMAAs with the substrate before encountering any other surface. The 57 amu profiles of Figure 1 indicate that most of these desorb, that is, follow reaction 1_r, a result consistent with a dynamic precursor-mediated synthesis to form the highly ordered and very hydrophobic TMA-covered surface.

The adsorption processes differ significantly for doses at 100 or 550 K, and much less is known about the structures formed and the organization of those structures. Thermal accommodation of the incident TMAA must be considered when the substrate is held at 100 K but should be very efficient, since both TMAA and TiO_2 have numerous low-frequency vibrational modes. Once accommodated, desorption (1_r) will occur at a negligible rate and, as observed, multilayer films will form readily, since 100 K lies below the multilayer TMAA desorption temperature (150 K). Thus, we expect the overall sticking coefficient to be near unity. Within the first adsorbed layer, deprotonation, process 3 or 4, likely occurs to some extent either during dosing or below 150 K in subsequent TPD.[18] However, for multilayer adsorption, the deprotonation reaction leads to a maximum TMA coverage that is one-third of that found for doses at 300 K. This indicates that, for multilayer doses formed at 100 K, as much as 0.4 ML of TMAA remains undissociated and in contact with the TiO_2(110) surface. During TPD, this undissociated TMAA desorbs before the temperature becomes high enough to meet the activation energy requirements for TMAA deprotonation that increase the TMA coverage via either reaction 3 or 4. For the submonolayer dose of TMAA that was used to generate the results depicted in Figure 8, we assume a surface comprised of TMA and OH was formed during dosing; that is, at this low coverage, all the adsorbed TMAA dissociated.

For doses at 550 K, energy sufficient to activate chemical reactions is transferred from TiO_2(110) to TMAA. A steady-

SCHEME 1: Trimethyl Acetate Interacting with TiO_2(110)

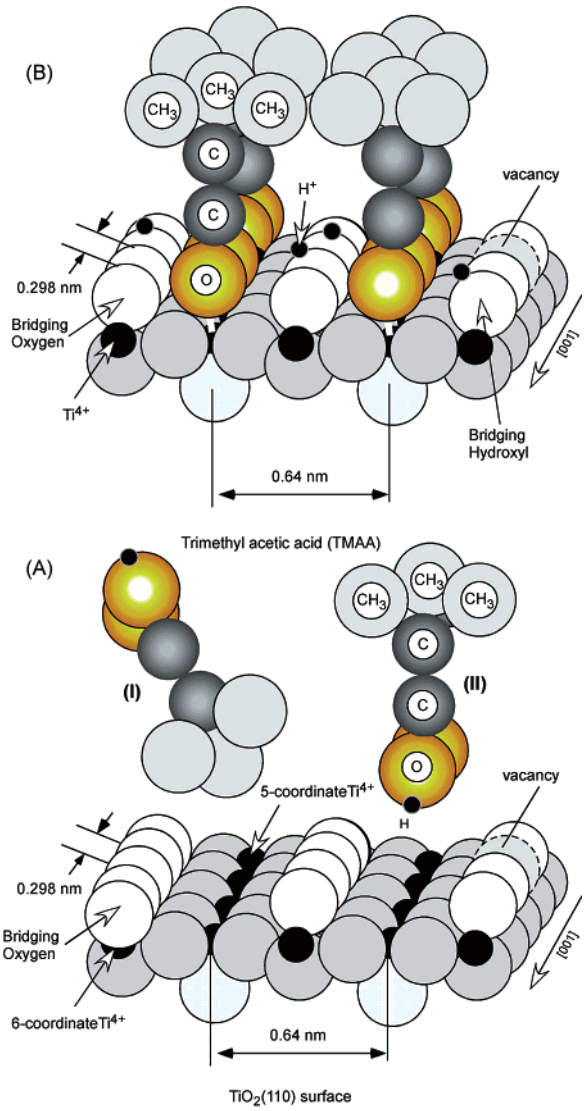

state reaction ensues with a surface composition consistent with a spatially averaged TMA coverage half that formed by saturation at 300 K. From the TPD of H_2O dosed at 100 K, after forming this coverage, the surface contains a high concentration of exposed Ti^{4+} that chemisorb water but there is no evidence for dissociative chemisorption, indicating that no bridging oxygen atom vacancies are present or that if present are either filled or blocked by TMA. We speculate that filling these vacancies gives rise to the transient H_2O and CH_4 profiles that appear on the approach to the steady-state reaction conditions depicted in Figure 2. In this regard, there is evidence (Figure 5) that lengthy photolysis of this surface leads to the formation of some OH, since a 460 K H_2O peak appears in TPD. Evidently, either some bridging oxygen atom vacancies become available or there is some photon-driven C−H bond breaking to protonate bridging oxygen atoms.

These results, coupled with the cleanliness of the TiO_2(110) surface after heating to 750 K or higher (for any dosing or photolysis conditions used here), are consistent with chemistry that does not lead to poisoning of sites that operate to convert adsorbed TMA and incident TMAA to products. On the basis of measurements made during dosing at 550 K (Figure 2), the steady-state reaction condition achieved involves the reaction of incident TMAA to form CO and H_2O at nearly equal rates (1:1 stoichiometry) and hydrocarbon species that do not passivate the TMAA dissociation sites. Thus, for doses at 550 K, we write an *overall* steady-state stoichiometry of

$$\mathrm{tBuCOOH_{(g)} \rightarrow [intermediates]_{(a\ and\ p)} \rightarrow CO_{(g)} + H_2O_{(g)} + C_xH_{y(g)}} \quad (5)$$

where intermediates designates a set of undetermined surface species and $C_xH_{y(g)}$ is a mixture of species dominated by *i*-C_4H_8 that is 60% of the CO. Besides *i*-C_4H_8, measurements made during dosing identify the production of *i*-C_4H_{10} and CH_4. The sum of *i*-C_4H_8 and *i*-C_4H_{10} is 75% of the CO. These estimates, while subject to considerable uncertainty (±15%), do indicate that gas-phase products, other than isobutene and isobutane, form and desorb during dosing at 550 K. These include CH_4 and, very likely, products identified in TPD, for example, 2,2,3,3-tetramethyl butane, $(tBu)_2$, methyl isopropenyl ketone, $(CH_3CH(CH_2)C(=O)CH_3)$, 2-butanone, 3-methyl, $((CH_3)_2CHC(=O)CH_3)$, and 1,3-butadiene, 2-methyl $(CH_2(CH_3)CCHCH_2)$.[7]

There is one additional interesting feature associated with dosing at 550 K, namely, the H_2O TPD peak slightly below 700 K. This desorption peak also appears in TPD after dosing TMAA at 100 and 300 K but is strongest for doses at 550 K. It does not appear for water dosed at 100 K. While there is no direct evidence regarding the path from TMAA to the species leading to this peak, we suggest that it may be the result of incorporation of H, and perhaps O also, into subsurface sites of TiO_2 during TMAA dosing at 550 K and during TPD following doses at 300 K. Since the surface is free of carbon following TPD, this peak does not appear to derive from C−H bond breaking at or above 650 K, to leave behind H-deficient carbon-containing species. For the surfaces photolyzed after a 550 K dose of TMAA, we assume the process is initiated at a surface covered with 0.3 ML of TMA species but few, if any, *surface* OH groups.

Photon-Driven Chemistry and Superimposed Thermal Chemistry. With the above thermal adsorption, desorption, and reaction considerations in mind, we now turn to the photochemistry. The photochemistry is initiated by photon absorption in the substrate, not by absorption in the adsorbate. This conclusion is consistent with the alterations of the electronic spectrum of TiO_2(110) that accompany the adsorbate photochemistry, namely, the appearance of a Ti^{3+} transition in the electronic electron energy loss spectrum.[15]

In simplified schematic terms,

$$\mathrm{TiO_2} + h\nu \rightarrow \mathrm{TiO_2} + \mathrm{h^+} + \mathrm{e^-} \qquad \text{(photon absorption)} \quad (6)$$

$$\mathrm{h^+} + \mathrm{e^-} \rightarrow \mathrm{heat} \qquad \text{(recombination)} \quad (7)$$

where the photon energy, $h\nu$, is sufficient (~3 eV) to promote an electron from the valence band to the conduction band of rutile. Photons are depleted by reaction 6 mainly within 1 μm of the surface, that is, a few times the wavelength. This depth scale is large compared to the scale of the unit cell of the single-crystal rutile substrate, ~1 nm. Since electron−hole recombination, reaction 7, is efficient, most of these excited carriers never reach the adsorbate−substrate interface and contribute nothing to the observed surface chemistry. This accounts for the very low upper limit of the product yield (10^{-5}) per incident photon that was estimated at the start of photolysis (where the rate is largest).

For the small fraction of holes and electrons formed at or arriving at the interface, reaction 7 occurs in competition with charge-transfer reactions involving the adsorbate, taken here to be a hole reaction with the adsorbed anion TMA.

$$\mathrm{h^+ + TMA \rightarrow TMA^*} \quad (8)$$

where TMA* represents an excited oxidized carboxylate. This oxidation can be thought of as extracting an electron from the π electron density of the carboxylate portion of TMA, a process that dramatically reduces the strength of the C−C bond between the carboxylate and *tert*-butyl groups of TMA. Oxidation of carboxyl groups is well-known in the literature[19] and leads to efficient decarboxylation: where $CO_{2(a)}^* + C_4H_{9(a)}^*$ are nascent

$$\mathrm{TMA^* \rightarrow CO_{2(a)}^* + C_4H_{9(a)}^*} \quad (9)$$

products presumed to be in nonequilibrium states in terms of internal energy and geometry. We take reaction 9 to be the primary photochemical step. Given the occurrence of reaction 9, subsequent steps follow paths that vary with substrate temperature and the energy deposited in the products. Thus, thermal chemistry follows the photochemistry.

Although not discussed here, earlier work shows that CO_2 production correlates linearly with the Ti^{3+} signal in electron energy loss spectra.[10] Thus, we assume that for every CO_2 molecule produced in reaction 9 an electron is localized (trapped) at the surface in a process that can be schematically represented as

$$\mathrm{e^- + Ti^{4+} \rightarrow Ti^{3+}} \quad (10)$$

where Ti^{3+} represents the trapped electron occupying a surface electronic state with an energy that lies in the band gap of bulk rutile. This state is kinetically stable at 300 K. As the concentration of trapped electrons increases, the following process competes with reaction 8 for holes:

$$\mathrm{Ti^{3+} + h^+ \rightarrow Ti^{4+}} \quad (11)$$

and inhibits decarboxylation, as observed. Other work[10] demonstrates that removing these trapped electrons by scavenging

with a short dose of O_2, that is, forming O_2^-, restores the decarboxylation rate.

If each TMA that reacts is accompanied by a trapped electron, it is of interest to consider the concentration of trapped electrons that would be present after photolyses with equal numbers of photons of surfaces prepared by dosing at different temperatures. For a saturation dose at 300 K, 1.1×10^{14} Ti^{3+}/cm^2 would be present. For photolyses at either 200 or 300 K after a 550 K dose, much less (6.2×10^{13} Ti^{3+}/cm^2) would accumulate. For both the 300 and 550 K doses, the quenched state involves about half the initial concentration of TMA. If the trapped electrons were free to move laterally, it is difficult to understand why the concentration required for quenching drops so strongly with the initial TMA concentration. Our observations are, on the other hand, consistent with a model involving lateral localization near the remaining TMA of those electrons trapped at the surface.[11] Empirically, this can be accounted for as

$$Ti^{3+} + TMA \rightarrow Ti^{3+}\cdots TMA \qquad (12)$$

According to this scheme, each time reaction 9 occurs, reaction 12 occurs and the resulting laterally localized $Ti^{3+}\cdots$TMA is no longer vulnerable to reaction 8 followed by reaction 9. As long as $Ti^{3+}\cdots$TMA is stable, the photolysis would be completely quenched when the initial concentration of TMA is reduced to half its initial value, as observed. Thus, we replace reaction 11 by reaction 12.

In prior STM work,[11] complementary evidence for lateral electron localization was presented and attributed to forming Ti^{3+} bound to a bridged hydroxyl group.

$$e^- + Ti^{4+}{-}OH^-{-}Ti^{4+} \rightarrow Ti^{4+}{-}OH^-{-}Ti^{3+} \qquad (13)$$

The present results for doses at 550 K suggest that refinement, as in reaction 12, of this picture is required because while there are very few bridging hydroxyl species present initially, quenching still occurs (Figure 6). Evidently, reaction 13 may occur but is not necessary for quenching.

Having accounted for the consumption of electrons and holes formed by photon absorption in the rutile, we return to a discussion of reaction 9. The nascent $CO_{2(a)}$* relaxes through two channels, reactions 14 and 15,

$$CO_{2(a)}^* \rightarrow CO_{2(g)} \qquad (14)$$

$$CO_{2(a)}^* \rightarrow CO_{2(p)} \qquad (15)$$

the former leading to ejection into the gas phase before thermal accommodation and the latter to thermally accommodated $CO_{2(p)}$. For photolysis at 100 K, evidence for reaction 14 is minimal, indicating that $CO_{2(a)}$* has a high probability of living long enough to thermally accommodate and be retained at the surface (Figure 6); that is, reaction 15 dominates reaction 14. Evidently, energy transfer to the substrate and, particularly on a crowded surface, to surrounding adsorbed species is rapid enough to accommodate the energy released in transforming the nonlinear O—C—O geometry of the carboxylate to the linear O═C═O product. Otherwise, CO_2 would not accumulate at the rate indicated during the first 10 min of photolysis (Figure 6).

For photolyses at 200 and 300 K, we presume that reaction 15 will still dominate over reaction 14, but since these temperatures lie above the desorption temperature of directly dosed CO_2, desorption will occur from $CO_{2(p)}$, the product of reaction 15 and, when the time resolution is of order 10° s as it is in Figures 9−11, will appear instantaneously; that is, reaction 16 is rapid.

$$CO_{2(p)} \rightarrow CO_{2(g)} \qquad (16)$$

Identifying the path followed by nascent *tert*-butyl, C_4H_9*, the second product of the primary photochemical event, is challenging, and many open questions remain. There is no evidence for desorption of this radical, and the delayed appearance of C_4 products (Figure 11) during photolysis at 200 K suggests thermalization, bonding, and thermal reactions of C_4H_9* dominate. The C_4H_9* radical is formed near the surface, has basic character, and presumably will bond with available Ti^{4+} cations, since these are acidic (reaction 17). The number of available Ti^{4+} will depend on the TMA coverage and, for a crowded surface, on whether C_4H_9 can create its own site by displacing other species, for example, CO_2 or TMA.

$$C_4H_9^* + Ti^{4+} \rightarrow Ti^{4+}{-}C(CH_3)_3 \qquad (17)$$

The chemisorbed product $Ti^{4+}{-}C(CH_3)_3$ is proposed to account for the thermal desorption of C_4 species between 275 and 300 K after photolysis at 100 or 200 K and for the *i*-C_4H_8 and *i*-C_4H_{10} desorbing during photolysis at 300 K (Figure 9). Rearrangement of $Ti^{4+}{-}C(CH_3)_3$ can account for *i*-C_4H_8.

$$Ti^{4+}{-}C(CH_3)_3 \rightarrow i\text{-}C_4H_{8(g)} + H_{(a)} \qquad (18)$$

The H from reaction 18 can be used to form *i*-C_4H_{10}

$$Ti^{4+}{-}C(CH_3)_3 + H_{(a)} \rightarrow i\text{-}C_4H_{10(g)} \qquad (19)$$

Here, it must be born in mind that *i*-$C_4H_{8(g)}$ exceeds *i*-$C_4H_{10(g)}$ by at least a factor of 5, so $H_{(a)}$ consumption channels other than reaction 19 must be in place. Migration beneath the surface is one possible channel for the consumption of $H_{(a)}$ and could contribute to the high-temperature (690 K) H_2O peak in TPD.

In the early stages of photolysis ($t \leq 10$ min in Figure 6) where the rate of photochemistry is being rapidly suppressed by the accumulation of Ti^{3+}, the following partial picture emerges. Photolysis at 100 K leads to rapid accumulation of $CO_{2(p)}$, Ti^{3+}, and $Ti^{4+}{-}C(CH_3)_3$. In subsequent TPD, physisorbed CO_2 follows desorption-limited kinetics, and $Ti^{4+}{-}C(CH_3)_3$ rearranges to form and desorb the reaction-limited *i*-butene (280 K) and *i*-butane (275 K). Photolysis at 200 and 300 K presumably follows the same paths, but additional thermal chemistry occurs at rates leading to product formation and desorption.

This picture is clearly incomplete, since it does not account for two desorption-limited peaks in TPD after photolysis at 100 K, namely, the *i*-butene peak at 190 K and the *i*-butane peak at 150 K. Evidently, there are paths to these physisorbed species that are open at all photolysis temperatures. The *i*-butene peak at 190 K grows rapidly in the first 10 min but saturates, likely tracking the quenching of the primary photolysis by Ti^{3+}. A plausible process to account for this is a photolysis step that occurs in parallel with reaction 9 to form two physisorbed species from TMA*.

$$TMA^* \rightarrow CO_{2(p)} + i\text{-}C_4H_{8(p)} + H_{(a)} \qquad (20)$$

When the production of TMA* is stymied by the accumulation of Ti^{3+}, the rate of reaction 20 becomes negligible.

The *i*-butane peak at 150 K differs from all of the other desorption peaks. It does not grow as rapidly as the others initially but continues to grow linearly with photolysis time even

after the accumulation of Ti^{3+} has reduced the TMA consumption rate to negligible values. During this period of time, the 280 K *i*-butene signal decays; thus, we speculate that these two may be linked by a secondary photon-driven reaction.

$$Ti^{4+}-C(CH_3)_3 + H_{(a)} + h\nu \rightarrow Ti^{4+} + i\text{-}C_4H_{10(p)} \quad (21)$$

Occurrence of reaction 21 at 100 K reduces the availability of $Ti^{4+}-C(CH_3)_3$ for reaction 18 in subsequent TPD. However, there is not a simple stoichiometric relation. On the basis of the integrated peak areas for *i*-butene and *i*-butane in these two peaks (Figure 6) for 10 and 90 min photolyses, $(2.4 \pm 0.2) \times 10^{13}$ cm^{-2} (0.05 ML) is added to the 150 K *i*-C_4H_{10} peak, while 10-fold less—$(2.3 \pm 1.2) \times 10^{12}$ cm^{-2} (0.004 ML)—is lost from the 280 K *i*-C_4H_8 peak. Adsorption from the background can be ruled out as the source of the linear increase of the 150 K *i*-C_4H_{10} intensity; after a series of dosing and photolysis experiments and a TPD to 750 K, the sample was cooled to 100 K and turned away from the incident photons that entered the chamber for 600 s (no chopper), that is, equivalent to 50 min with the chopped source. The substrate temperature did not rise during this period, and there was no detectable 150 K 43 amu peak in subsequent TPD. Thus, there is a photon-driven process that steadily produces 5×10^9 cm^{-2} s^{-1} of physisorbed *i*- C_4H_{10} over the full 90 min time range of Figure 6. Accounting for the 16% duty cycle of the chopped source and 10^{17} photons/s when the source is supplying light, the yield is very low, 3×10^{-7} $photon^{-1}$.

One proposal consistent with these observations maintains a link between reactions 18 and 21 as follows. When reaction 21 occurs, the $Ti^{4+}-C(CH_3)_3$ consumed can, with low probability, be replaced by the slow occurrence of the sequence reaction 8, reaction 9, and reaction 17. As a result, the amount of *i*-C_4H_8 lost from the 285 K peak is less than the amount gained by the 150 K *i*-C_4H_{10} peak.

6. Summary

Surfaces prepared by dosing trimethyl acetic acid (TMAA) onto clean annealed rutile TiO_2(110) at 100, 300, and 550 K were photolyzed in an anaerobic UHV environment at 100, 200, and 300 K. Products formed and desorbed during dosing and irradiation were monitored by isothermal mass spectrometry (ISOMS). Temperature programmed desorption (TPD) spectra taken with and without photolysis were compared to assess changes in surface concentrations and composition driven by photons. Dosing TMAA at 300 K is described in terms of adsorption into a mobile precursor state that either desorbs or deprotonates to form trimethyl acetate (TMA), the latter process occurring preferentially adjacent to already existing TMA. Defining 1 monolayer (ML) as the number of exposed Ti^{4+} cations on a perfect (110) rutile surface, the saturation TMA coverage is 0.6 ML. This coverage exceeds 0.5 ML, the value expected for the (2×1) structure observed in earlier STM work, and is accounted for in terms of some relatively weakly held chemisorbed TMAA that would not be imaged in STM. Deprotonation associated with dosing at 100 K is limited, and TPD of multilayers gives 0.2 ML as the maximum amount of TMA formed. Dosing at 550 K leads to steady-state kinetics that is characterized by a TMA coverage of 0.3 ML. Photolysis of these TMA-covered surfaces is initiated by UV absorption in the rutile, a process that forms electron−hole pairs. The photon-driven chemistry is characterized by rapid initial hole-initiated decarboxylation rates of TMA to form CO_2 and adsorbed *tert*-butyl radicals (*tert*-$butyl_{(a)}$), the latter accommodating thermally, bonding to the Ti^{4+} cations and either accumulating if the temperature is below 300 K or undergoing thermal reactions to form and desorb mainly isobutene (*i*-C_4H_8) along with some isobutane (*i*-C_4H_{10}) if the photolysis temperature is 300 K. For lengthy photolysis at 100 K, there is evidence for a slow secondary photon-driven reaction of *tert*-$butyl_{(a)}$ to form physisorbed *i*-C_4H_{10}. For all cases, the rate of photolysis is rapidly quenched, an effect attributed to the trapping and lateral localization of electrons adjacent to remaining TMA forming spatially localized $Ti^{3+}-$TMA, a species that does not decarboxylate in the presence of a hole.

Acknowledgment. M.A.H. and J.M.W acknowledge support by the U.S. Department of Energy, Office of Basic Energy Sciences, Division of Chemical Sciences. J.M.W. also acknowledges support from the Center for Materials Chemistry at the University of Texas at Austin and the Robert A. Welch Foundation. Pacific Northwest National Laboratory is a multiprogram national laboratory operated for the U.S. Department of Energy by the Battelle Memorial Institute under contract DE-AC06-76RLO1830. Part of the research reported here was performed in the William R. Wiley Environmental Molecular Science Laboratory, a Department of Energy user facility funded by the Office of Biological and Environmental Research.

References and Notes

(1) Linsebigler, A. L.; Lu, L.; Yates, J. T., Jr. *Chem. Rev.* **1995**, *95* (3), 735−758.
(2) Fujishima, A.; Rao, T. N.; Tryk, D. A. *J. Photochem. Photobiol.* **2000**, *1* (1), 1−21.
(3) Kudo, A. *Catal. Surv. Asia* **2003**, *7*, 31−38.
(4) Wang, R.; Hashimoto, K.; Fujishima, A.; Chikuni, M.; Kojima, E.; Kitamura, A.; Shimohigashi, M.; Watanabe, T. *Nature* **1997**, *388*, 431.
(5) Mills, A.; Davies, R. H.; Worsley, D. *Chem. Soc. Rev.* **1993**, *22*, 417−425.
(6) Hagfeldt, A.; Graetzel, M. *Acc. Chem. Res.* **2000**, *33*, 269−277.
(7) White, J. M.; Szanyi, J.; Henderson, M. A. *J. Phys. Chem. B* **2004**, *108*, 3592−3602.
(8) White, J. M.; Szanyi, J.; Henderson, M. A. *J. Phys. Chem. B* **2003**, *107*, 9029−9033.
(9) White, J. M.; Henderson, M. A.; Uetsuka, H.; Onishia, H. *Proc. SPIE, Physical Chemistry of Interfaces and Nanomaterials III* **2004**, *5513*, 66−75.
(10) Henderson, M. A.; White, J. M.; Uetsuka, H.; Onishi, H. *J. Am. Chem. Soc.* **2003**, *125*, 14974−14975.
(11) Uetsuka, H.; Onishi, H.; Henderson, M. A.; White, J. M. *J. Phys. Chem. B* **2004**, *108*, 10621−10624.
(12) Onishi, H. *Catal. Surv. Jpn.* **2002**, *6*, (1/2).
(13) Henderson, M. A.; White, J. M. Manuscript in preparation, 2005.
(14) Henderson, M. A. *Surf. Sci.* **1996**, *355*, 151.
(15) Diebold, U. *Surf. Sci. Rep.* **2003**, *48*, 53−229.
(16) Estimated by measuring intensities with an external optical power meter and adjusting for reflection of window at vacuum wall.
(17) Henderson, M. A. *Surf. Sci. B* **1998**, *400*, 203.
(18) Henderson, M. A. *J. Phys. Chem. B* **1997**, *101*, 221.
(19) Kraeutler, B.; Bard, A. J. *J. Am. Chem. Soc.* **1978**, *100*, 2239−2240.